A&A 377, 44–51 (2001)
DOI: 10.1051/0004-6361:20011014

Astronomy & Astrophysics

BeppoSAX observations of the Narrow-Line Seyfert 1 galaxy RX J1702.5+3247

M. Gliozzi[1], W. Brinkmann[1], S. A. Laurent-Muehleisen[2,⋆], E. C. Moran[3], and J. Whalen[2]

[1] Max-Planck-Institut für extraterrestrische Physik, Postfach 1312, 85741 Garching, Germany
[2] Department of Physics, University of California–Davis, 1 Shields Ave., Davis, CA 95616, USA
[3] Department of Astronomy, University of California, Berkeley, CA 94720 USA

Received 23 February 2001 / Accepted 5 July 2001

Abstract. We report optical, radio and X-ray observations of the Narrow-Line Seyfert 1 galaxy RX J1702.5+3247. The soft (0.1–2 keV) X-ray flux, measured by BeppoSAX, is characterized by strong variability on short time scales (<500 s). The most extreme amplitude variations require a radiative efficiency exceeding the maximum for a Kerr black hole, implying the presence of relativistic effects. A comparison with archival ROSAT data reveals long term temporal and spectral variability. The 0.1–10 keV spectrum is equally well fitted either by an ionized reflection disk model, or by a broken power law plus a Gaussian line, consistent with a hydrogen–like iron line at 6.97 keV from a highly ionized accretion disk.

Key words. galaxies: active – galaxies: fundamental parameters – galaxies: nuclei – X-rays: galaxies

1. Introduction

Narrow-line Seyfert 1 galaxies (NLS1; see Osterbrock & Pogge 1985) are a peculiar class of AGN defined by their optical line properties: the Hβ FWHM does not exceed 2000 km s^{-1}, the [O III]λ5007 to Hβ ratio is less than 3, and the UV−visual spectrum is usually rich in high-ionization lines and strong Fe II emission multiplets.

ROSAT and ASCA observations have shown that the X-ray properties of NLS1 galaxies are remarkably different from those of "normal" Seyfert 1 galaxies. Large amplitude X-ray variability with time scales as short as few hundred seconds (Forster & Halpern 1996; Boller et al. 1997; Brandt et al. 1999) and very steep soft X-ray spectra (Boller et al. 1996) are common among these objects. On average, NLS1 galaxies have steeper energy spectra also in the hard 2–10 keV energy band (Brandt et al. 1997) and show higher variability (Fiore et al. 1998; Leighly 1999a). A clear anti-correlation between the soft X-ray spectral slope and the Hβ FWHM has been found over a wide range of X-ray luminosities (Boller et al. 1996; Laor et al. 1997). Emission lines of highly ionized iron have been discovered in several NLS1 galaxies (Pounds et al. 1995; Comastri et al. 1998; Turner et al. 1998; Leighly 1999b). This supports the hypothesis of the presence of a particularly high accretion rate in NLS1 galaxies (Pounds et al. 1995), as the ionization parameter scales with $(\dot{M}/\dot{M}_{\rm Edd})^3$ (Ross & Fabian 1993).

NLS1 are rarely radio-loud (Remillard et al. 1991; Ulvestad et al. 1995; Siebert et al. 1999; Grupe et al. 2000), and thus their radio properties have been poorly explored. An unexpectedly large number of NLS1 has been discovered among the sources found in the cross correlation of the ROSAT All Sky Survey (RASS) and the FIRST VLA radio survey (Brinkmann et al. 2000; Becker et al. 1995). Although NLS1 galaxies have become a topical subject of AGN research, a general picture explaining the peculiar optical and X-ray properties has not yet emerged. An important question is how the properties of NLS1 galaxies depend on the orientation of the sources with respect to the line of sight. The presence of radio emission and the associated relativistic jet in radio-loud NLS1 galaxies might provide us with a handle on the orientation issue. Originally it was suggested that NLS1 are the pole-on versions of normal Seyfert 1 galaxies. This hypothesis can explain many of the NLS1 properties, namely the narrower permitted lines, the strong Fe II emission, the low frequency of warm absorbers and the rapid variability. On the other hand the orientation model is in contrast with slab thermal Comptonization models (e.g. Haardt & Maraschi 1993), which predict softer spectra as the

Send offprint requests to: M. Gliozzi,
e-mail: mgliozzi@xray.mpe.mpg.de

⋆ Visiting Astronomer, Kitt Peak National Observatory, National Optical Astronomy Observatories, which is operated by the Association of Universities for Research in Astronomy, Inc. (AURA) under cooperative agreement with the National Science Foundation.

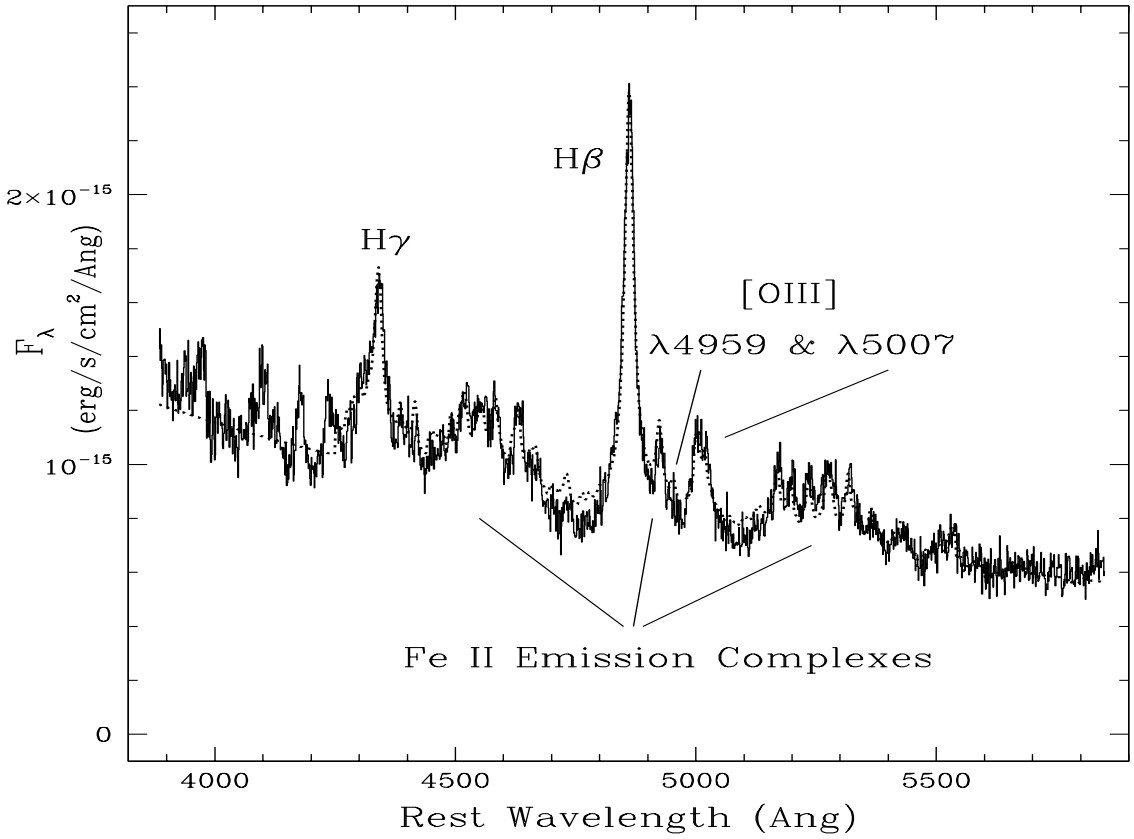

Fig. 1. A blow up of the 3880–5850 Å region in the observed broad band spectrum of RX J1702.5+3247. The spectrum was taken on 4 June, 1997, and has a resolution of 3.7 Å. Because observing conditions were not photometric, the flux scale shown on the left should be used only as a rough guide to the actual source brightness. The solid line shows the observed (but deredshifted) spectrum while the dotted line shows the fit described in the text. Labeled are the [OIII], Hβ and Hγ lines as well as the strong Fe II emission complexes.

inclination angle increases. However, if the hot phase responsible for the Comptonization is contained in discrete regions (blobs) above the disk, the X-ray spectral index depends mainly on the geometry of the blobs rather than on the inclination of the disk (Haardt et al. 1994).

In this paper we present the X-ray observations both from BeppoSAX and ROSAT of RX J1702.5+3247 [RA(2000) = $17^{\rm h}02^{\rm m}31^{\rm s}$, DEC(2000) = $+32^{\rm o}47'20''$; $z = 0.163$], together with optical and radio observations. Throughout the paper we use a Friedman cosmology with $H_0 = 70\ {\rm km\,s^{-1}\,Mpc^{-1}}$ and $q_0 = 0.5$ for the computation of the K-corrected luminosities.

2. Radio and optical observations

RX J1702.5+3247 is a radio-selected source from the FIRST (Faint Images of the Radio Sky at Twenty centimeters; Becker et al. 1995) radio survey. It is an unresolved radio point source with a peak flux of 1.8 mJy. An optical counterpart was found on the POSS plates with a blue magnitude of $m_{\rm O} = 15.7$ and a red magnitude of $m_{\rm E} = 15.8$. This object is a member of the FIRST Bright Quasar Survey (FBQS; White et al. 2000) and was observed spectroscopically on June 4, 1997, with GoldCam on the Kitt Peak 2.1-m telescope. The dispersion was 1.5 Å/pix. All sources with even moderately broad optical emission lines, including RX J1702.5+3247, were classified as quasars in the FBQS. Our analysis of the optical spectrum (Fig. 1) shows that it can more precisely be classified as a Narrow Line Seyfert 1 galaxy.

We fitted the optical continuum from 3700 to 6000 Å using the SPECFIT routine in the IRAF (v. 2.11.3) data analysis package. The spectrum was not taken under photometric conditions, so we restrict our analysis to parameters insensitive to the absolute flux scale. The Hβ line was fit with a Lorentzian profile and has a width of $\sim$1400 km s^{-1}. The [OIII] lines were also fit with Gaussian profiles with widths that were $\sim$650 km s^{-1}. This is very close to the resolution of our dataset, so a higher resolution spectrum is required to determine the true [OIII] line widths. The Fe II emission was fit using the template from Boroson & Green (1992) which was derived from IZw1. Our spectrum does not extend far enough to the red to measure the [NII] or Hα lines. In the region localized to the Fe II emission, Hβ and [OIII] lines, we find the continuum is well parameterized as a power law with a slope of $\alpha = 1.9$ ($S_\lambda \propto \lambda^{-\alpha}$). Similar parameters are reported

by Bade et al. (1995). These characteristics taken as a whole exhibit all the classical features of a NLS1 galaxy: the Fe II emission is strong compared to a normal Seyfert galaxy and the [OIII] and Hβ emission are both narrow and strong, although the [O III] to Hβ flux ratio (0.04) is remarkably weak in this object.

The redshift of the source is $z = 0.163$ [1], which yields a monochromatic radio luminosity of 1×10^{30} erg s^{-1} Hz^{-1}. We also find that the K-corrected radio-to-optical flux ratio, R^* (following the definition in Stocke 1992), is 1.2 [2]. Clearly this source is radio-quiet (as are most presently known NLS1s). Nevertheless, it is radio-selected and may possess small-scale, possibly relativistic, jets as has recently been reported in some Seyfert galaxies (see below).

3. X-ray observations and data reduction

RX J1702.5+3247 was first observed with the ROSAT (Trümper 1983) Position Sensitive Proportional Counter (PSPC, Pfeffermann et al. 1986) during the ROSAT All-Sky Survey (Voges et al. 1999) on two occasions, namely on August 18, 1990 and February 17, 1991, with exposures of 810 s and 306 s, respectively. Further, on August 3, 1993 RX J1702.5+3247 was serendipitously observed during a PSPC pointed observation of the cluster of galaxies Abell 2241, with an exposure of ∼11 ks. The analysis of the ROSAT data were performed using the EXSAS data analysis package (Zimmermann et al. 1996). For the pointed observation, the light curve and spectrum were extracted from a circle with a 300″ radius around the source center; the background was taken from a ring centered on the source with inner and outer radii of 400″ and 500″, respectively.

RX J1702.5+3247 was observed with the BeppoSAX (Boella et al. 1997a) Narrow Field Instruments: LECS (0.1–10 keV; Parmar et al. 1997) and MECS (1.3–10 keV; Boella et al. 1997b) on March 9–10, 2000 with effective exposures of 16.0 ks and 38.3 ks, respectively. The shorter LECS exposure resulted from the instrument being switched off over the illuminated Earth. The observations were performed with 2 active MECS units (after the failure of MECS1 on May 6, 1997). Standard data reduction techniques were employed following the prescription given by Fiore et al. (1999). LECS and MECS spectra and light curves were extracted from regions with radii of 8 arcmin and 4 arcmin respectively, in order to maximize the accumulated counts at both low and high energies. Background spectra were extracted from high Galactic latitude "blank" fields, whereas for the light curves a source-free region in the field of view was used. The background subtracted count rates are $(3.83 \pm 0.22) \times 10^{-2}$ cts s^{-1} and $(2.15 \pm 0.09) \times 10^{-2}$ cts s^{-1} for LECS and MECS respectively.

[1] This redshift differs from that reported in NED by 0.001 ($z_{\rm NED} = 0.164$). Our redshift is taken from White (et al. 2000), who determined their redshifts by cross-correlating spectra with a quasar template, effectively taking a global average over all the lines and features in the observed spectrum.

[2] Both the monochromatic radio power and R^* are calculated at 1.4 GHz instead of the standard 5 GHz. If the radio spectral index is steeper than zero, both the radio power and R^* will be less than the values reported above.

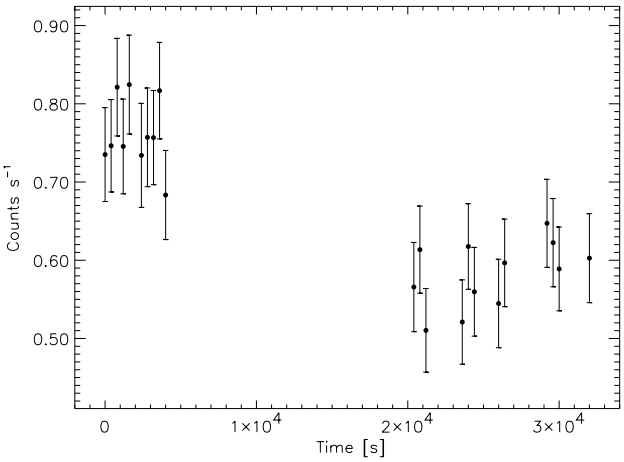

Fig. 2. ROSAT PSPC light curve on August 3, 1993. Every data point corresponds to 400 s integration time.

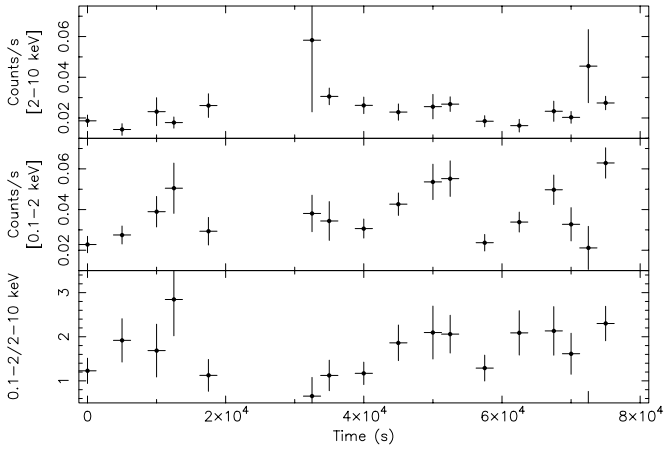

Fig. 3. MECS (top panel), LECS (middle panel) and soft-to-hard counts ratio (bottom panel) of RX J1702.5+3247 on March 9–10, 2000, with time binning of 2500 s.

4. Temporal analysis

The short exposures during the RASS do not permit a detailed temporal analysis. On the other hand, the availability of two observations taken six months apart allows us to look for long term variability. Indeed, the average count rate changed by a factor ∼3, increasing from 0.35 ± 0.20 cts/s on August 18, 1990 to 1.13 ± 0.41 cts/s on February 17, 1991. There is also evidence for long term spectral variability: the source spectrum becomes softer as the flux increases (Grupe et al. 2001). Figure 2 shows the ROSAT PSPC light curve on August 3, 1993 during the pointed observation. An integration time of 400 s per bin was used in order to obtain good statistics and avoid count rate variations due to the ROSAT wobble. Figure 2 shows that RX J1702.5+3247 was moderately variable during the pointed observation with count rate changes as large as 40% in a few hours.

In Fig. 3 the LECS and MECS light curves with time binning of 2500 s are shown, together with the corresponding [0.1–2 keV]/[2–10 keV] soft-to-hard counts ratios. While the MECS light curve is basically consistent with the hypothesis of constant flux (the χ^2 probability that the flux is constant is $p \sim 0.9$), variability up to a factor of 2 on time scales of hours is detected in the LECS light curve with a high level of confidence ($p < 3 \times 10^{-4}$). There is also evidence of spectral variability. Since the flux is dominated by the soft photons, the softness ratio follows the low energy light curve, and the spectrum softens when the total flux increases.

A characteristic property exhibited by several NLS1 galaxies is the presence of large flares on very short time scales. Figure 4, which shows the LECS light curve with 500 s binning, reveals the presence of significant variability ($p < 0.15$) on shorter time scales, namely within the individual orbits, while the background count rate remains basically constant. In particular, around $t = 7.5 \times 10^4$ s, the source count rate varies by a factor of 4 in 500 s. We therefore investigated the LECS light curve with even smaller binning (100 s), and found that in at least four orbits there is evidence of strong variability on very short time scales. For brevity we concentrate on orbit 13 (using the data between $t = 7.59 \times 10^4$ s and $t = 7.67 \times 10^4$ s after the beginning of the observation), which contains the largest number of data points during a flare (see Fig. 5). We performed a linear least square fit to determine the count rate variations during the rise and the decline of the flare and found $\Delta\mathrm{rate}/\Delta t = (2.28 \pm 0.75) \times 10^{-4}$ cts s^{-2} and $\Delta\mathrm{rate}/\Delta t = (2.06 \pm 0.27) \times 10^{-4}$ cts s^{-2}, respectively. We calculated the corresponding luminosity variations in the rest frame of RX J1702.5+3247 by assuming a power law spectral model with the best fit parameters (discussed in Sect. 5) of the 0.1–2 keV LECS spectrum. We obtained $\Delta L_{0.1-2\ \mathrm{keV}}/\Delta t = (5.1 \pm 1.7) \times 10^{42}$ erg s^{-2} for the rise and $\Delta L_{0.1-2\ \mathrm{keV}}/\Delta t = (4.6 \pm 0.6) \times 10^{42}$ erg s^{-2} for the decay, which are extremely high values, even for NLS1 galaxies. We are aware that the small number of data points yield a less than robust statistical significance. On the other hand, the presence of similar short flares in different orbits supports the hypothesis of strong variability. For a firm confirmation we have to await further observations from the new X-ray missions such as XMM-Newton, with sensitive, high time resolution instruments and the possibility of long continuous observations.

The luminosity variations can be used to estimate the lower limit of the radiative efficiency: $\eta > 4.8 \times 10^{-43} \Delta L/\Delta t$ (Fabian 1979). Straightforward application of this relation gives $\eta > 2$ for both the rise and the decay. This suggests that some assumptions used in the calculation of the efficiency limit must be relaxed, allowing uniform radiation release and relativistic effects in the vicinity of the black hole (e.g. Brandt et al. 1999). Interestingly, a similar extreme value for the efficiency was derived by Remillard et al. (1991) from the Ginga 2–10 keV observation of PKS 0558–504, a radio-loud NLS1 galaxy.

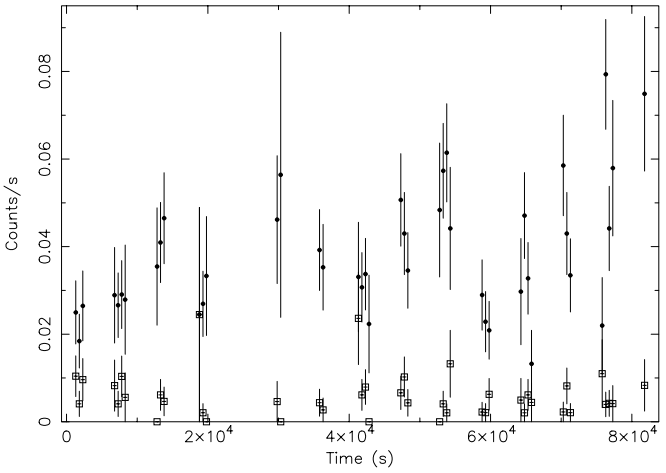

Fig. 4. LECS light curve. Every data point corresponds to 500 s integration time. Filled circles and open squares represent the source and the background count rates, respectively.

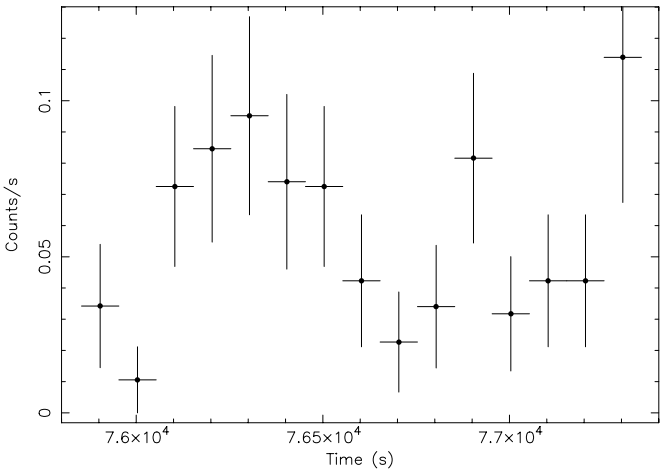

Fig. 5. LECS light curve of orbit 13. Every data point corresponds to 100 s integration time.

We compared the ROSAT PSPC count rate with the LECS, by using W3PIMMS with a power law model and the best fit parameters ($\Gamma = 3.37$, $N_{\mathrm{H}} = 2.47 \times 10^{20}$ cm^{-2}) of the PSPC spectrum during the pointed observation. The average count rate of 6.6×10^{-1} cts s^{-1}, found with the PSPC on August 3, 1993, corresponds to 3.85×10^{-2} cts s^{-1} in the 0.1–2 keV energy band of the LECS, which is consistent with the average rate of 3.83×10^{-2} cts s^{-1} measured in March 2000.

5. Spectral analysis

5.1. Spectral fitting

Spectra from the ROSAT data were produced using the standard procedures from the EXSAS analysis package. Source counts were binned to give a minimum signal to noise ratio of $\geq$5. The poor photon statistics of the spectrum of RX J1702.5+3247, obtained from the RASS data, do not allow sophisticated fits. A power law plus

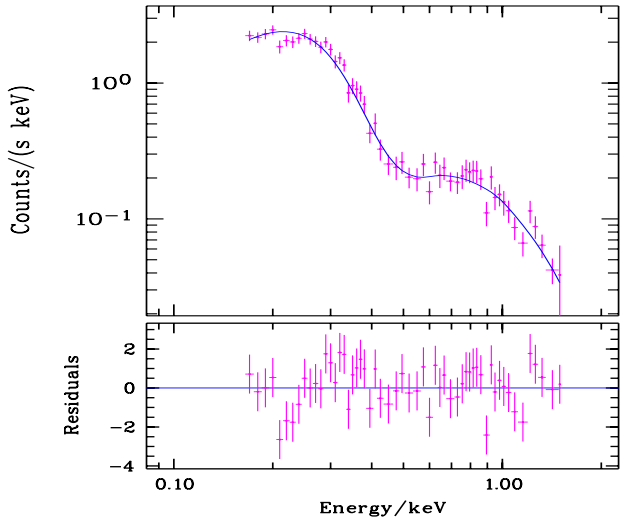

Fig. 6. Single power law fit of the ROSAT PSPC pointed observation with $N_{\rm H}$ fixed to the Galactic value for RX J1702.5+3247; top panel the folded spectrum, bottom panel the residuals.

absorption model reveals that the intrinsic absorption in the source is negligible and therefore we fixed the absorption at the Galactic value ($N_{\rm H} = 2.47 \times 10^{20}$ cm^{-2}; Dickey & Lockman 1990). The resulting best fit parameters are $\Gamma = 3.13 \pm 0.14$ and $\chi^2 = 9.4$ (12 d.o.f.). Figure 6 shows that also during the PSPC pointed observations a single power law fit with column density fixed to the Galactic value is an acceptable description ($\chi^2 = 62.2$ for 54 d.o.f.) for the soft spectrum. The results of the spectral fits assuming Galactic absorption are summarized in Table 1. On the basis of the best fit model, the unabsorbed 0.1–2.4 keV flux is 1.8×10^{-11} erg cm^{-2} s^{-1}, corresponding to a soft X-ray luminosity of 1.4×10^{45} erg s^{-1} (on August 3, 1993).

For the spectral analysis of the BeppoSAX data we used the XSPEC 10 software package and the latest release of the response matrices. LECS and MECS spectra were rebinned in order to have at least 20 counts per energy channel. Due to the slight mis-match in the cross-calibration of the different detectors, it has become necessary to include multiplicative factors for the normalization of the fitted models. The correct absolute flux normalization is provided by the MECS and the expected value of these constant factors is well known (between 0.7 and 1) and does not constitute an additional source of uncertainty (Fiore et al. 1999). In the following, all quoted errors correspond to 90% confidence levels.

A summary of the individual LECS and MECS datasets fitted with a single power law plus Galactic absorption is reported in Table 1. Leaving the column density free to vary, one gets similar results with a best fit value of $N_{\rm H} = (1.85 \pm 0.8) \times 10^{20}$ cm^{-2}, consistent with the Galactic value. The relatively poor fit of the MECS spectrum can be ascribed to the presence of line-like excess emission around 7 keV.

Table 1. Single power law fits with fixed Galactic absorption.

Instrument	Γ	χ^2/d.o.f.	$\chi^2_{\rm red}$
PSPC (RASS)	3.13 ± 0.14	9.4/12	0.78
PSPC (pointed)	3.37 ± 0.05	62.2/54	1.15
LECS	2.94 ± 0.10	40.02/37	1.14
MECS	2.43 ± 0.20	48.08/35	1.37

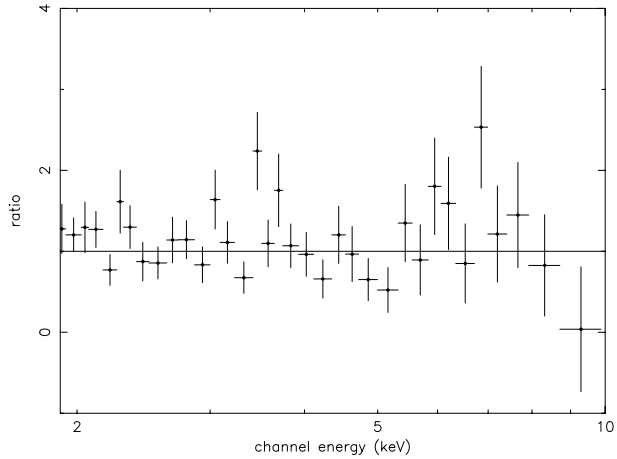

Fig. 7. Data to model ratio for the power law fit to the 2–10 keV MECS spectrum.

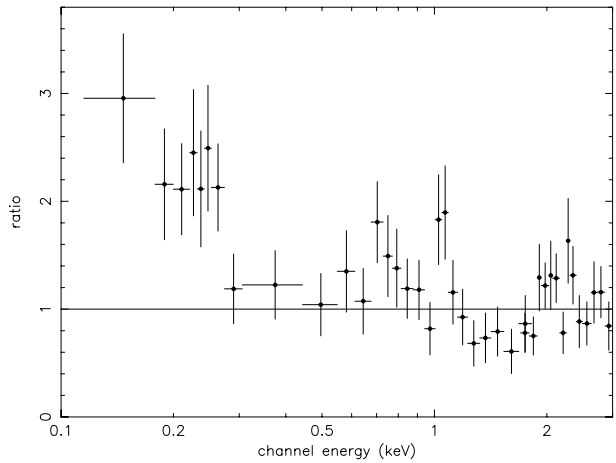

Fig. 8. Data to model ratio given a power law fit to the 2–10 keV spectrum.

By extrapolating the power law model fitted in the 2–10 keV band down to 0.1 keV (Fig. 8), a soft component is revealed, but only at very low energies below 0.3 keV.

A simultaneous fit of a power law model with fixed Galactic absorption to the LECS (restricted to the range 0.1–2 keV, to avoid the large errors at higher energies) and MECS data resulted in a slope of $\Gamma = 2.81 \pm 0.11$ and a relatively poor $\chi^2 = 87.88$ (61 d.o.f.). A statistically significant improvement of the fit ($\Delta\chi^2 = 5.68$, significant at more than 90% confidence for two additional free parameters) is achieved by adding a Gaussian line

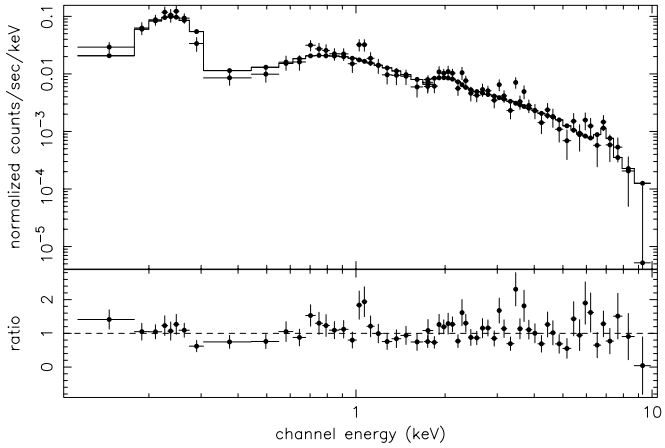

Fig. 9. LECS and MECS spectrum of RX J1702.5+3247 with a broken power law model plus a Gaussian line superimposed.

profile to the power law model. In order to determine the line parameters, given the quality of the data, the energy centroid of the Gaussian was constrained to lie in the range 5.5–7.5 keV and its width was fixed at 0.1 keV. The resulting line is centered at $7.11^{+0.32}_{-0.28}$ keV in the rest frame, and has an equivalent width of 804^{+856}_{-511} eV. Such a high value for the equivalent width is not uncommon among NLS1 galaxies: similar values were reported for Ton S 180 ($EW = 507 \pm 247$ eV, Comastri et al. 1998) and PG 1244+026 ($EW = 594$ eV, Ballantyne et al. (2001)). We also tried to fit the data with a power law plus a relativistic disk line (Laor 1991), however, neither a significant improvement of the fit nor a more accurate determination of the line parameters was achieved.

We therefore tried more complex two-component models which are currently used to fit the broad band X-ray spectra of NLS1 galaxies (e.g. Leighly 1999b): a blackbody model superimposed on a simple power law, a bremsstrahlung model plus a power law, and a broken power law. Only the latter gave a statistically significant improvement of the fit: the difference in χ^2 is significant at more than 99.9% confidence, according to an F–test. An even better fit (at confidence level between 68% and 90%) is obtained by adding a Gaussian line. The resulting fit, superimposed on the data, is shown in Fig. 9. All LECS+MECS joint fits are summarized in Table 2. On the basis of the best fit model, the unabsorbed 0.1–2.4 keV flux is 1.18×10^{-11} erg cm^{-2} s^{-1}, corresponding to a soft X-ray luminosity of 8.5×10^{44} erg s^{-1}. The 2.4–10 keV flux is 0.9×10^{-12} erg cm^{-2} s^{-1}, corresponding to a hard X-ray luminosity of 6.4×10^{43} erg s^{-1} is roughly a factor 13 lower than the soft one.

5.2. Ionized disk models

Stimulated by very recent spectral results on ASCA data of NLS1 galaxies (Ballantyne et al. (2001)), where the ionized reflection model (Ross & Fabian 1993; Ross et al. 1999) proved to provide excellent fits to the data, we performed a similar analysis on the SAX data. In this model, the accretion disk is approximated as a slab of gas with constant density ($n_{\rm H} = 10^{15}$ cm^{-3}) and solar abundances, which is illuminated by an X-ray flux $F_{\rm x}$, described by a power law with photon index Γ. The reflected spectrum is multiplied by R, the reflected fraction, and then added to the incident spectrum to give the resulting observed spectrum. The structure of the reflected spectrum is determined by the ionization parameter ξ, which varies as a function of the incident flux. Recently, Nayakshin et al. (2000) presented more sophisticated ionized reflection models, where the density is determined from hydrostatic balance, which is solved simultaneously with ionization balance and radiative transfer. The authors point out that, due to a thermal instability, only a very thin layer at the top of the slab is highly ionized, and the reflected spectrum is dominated by the neutral material underneath. However, in case of a steep ($\Gamma > 2$) incident spectrum, as typical for NLS1 galaxies, the Nayakshin et al. model predicts the presence of an ionized region of substantial optical depth and therefore ionized features superimposed on the emerging X-ray spectrum. Thus, despite the simplifying assumption of constant density, the use of the Ross & Fabian ionized reflection model is justified in the case of the steep spectrum NLS1 galaxy RX J1702.5+3247. Further it is preferable to the alternative ionized disk model (PEXRIV) adapted in the XSPEC spectral fitting procedures, for its capacity to fit simultaneously the continuum and the superimposed lines. Figure 10 shows the best fit ionized disk model ($\Gamma = 2.56$, $\log \xi = 3.4$, $R = 0.94$). The fit parameters are consistent with those found for Ton S 180 by Ballantyne et al. (2001), although the reflection fraction R of RX J1702.5+3247 is poorly constrained.) The most prominent feature is the Fe Kα line at 5.9 keV in the observer rest frame, which corresponds to a rest frame energy of 6.9 keV, in full agreement with the fluorescent emission from H-like Fe ions. The ionized disk model fits the Fe line and the continuum simultaneously and thus determines the Fe Kα centroid energy, but no further information on the line parameters is provided. The ratio between data and model, shown in Fig. 11, demonstrates that the ionized disk model gives an acceptable representation of the spectrum over the entire energy range. A comparison between the ionized disk model and the broken power law plus a Gaussian line indicates that the latter is not preferable, since a $\Delta\chi^2 = 2.6$ is significant at less than 68% confidence level for three additional free parameters. Moreover, for both models we calculated the probability to find a better reduced χ^2 given the respective χ^2 and degrees of freedom. The result shows that the ionized disk model and the broken power law plus a Gaussian line cannot be discriminated at a confidence level of 99%.

6. Discussion

The X-ray properties of RX J1702.5+3247 are remarkable, both in the temporal and spectral behaviour.

Table 2. LECS+MECS joint fits to the 0.1–10 keV continuum. All values quoted are in the rest frame.

Model	Γ_1	$E_{\rm br}$(keV)	Γ_2	$E_{\rm line}$(keV)	EW (eV)	χ^2/d.o.f.	$\chi^2_{\rm red}$
pow	$2.81^{+0.11}_{-0.11}$					87.88/61	1.44
po+ga	$2.83^{+0.11}_{-0.11}$			$7.11^{+0.32}_{-0.28}$	804^{+856}_{-511}	82.20/59	1.39
bkn	$2.93^{+0.14}_{-0.13}$	$1.7^{+0.8}_{-0.6}$	$2.45^{+0.19}_{-0.22}$			77.09/59	1.30
bkn+ga	$2.92^{+0.14}_{-0.12}$	$1.62^{+0.82}_{-0.57}$	$2.50^{+0.20}_{-0.21}$	$8.08^{+0.55}_{-1.18}$	808^{+682}_{-758}	73.94/57	1.30

Model	Γ	$\log \xi$	R	χ^2/d.o.f.	$\chi^2_{\rm red}$
refl disk	$2.56^{+0.13}_{-0.12}$	$3.40^{+0.35}_{-0.31}$	$0.94^{+0.86}_{-0.57}$	76.54/60	1.27

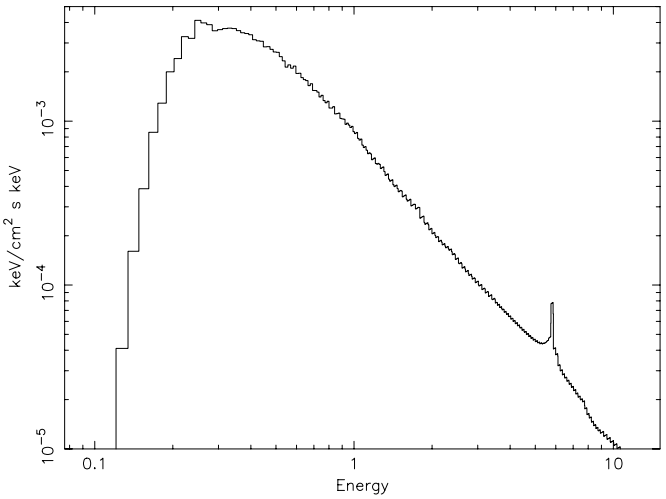

Fig. 10. Best fit ionized disk model for RX J1702.5+3247. The energy is in the observer frame.

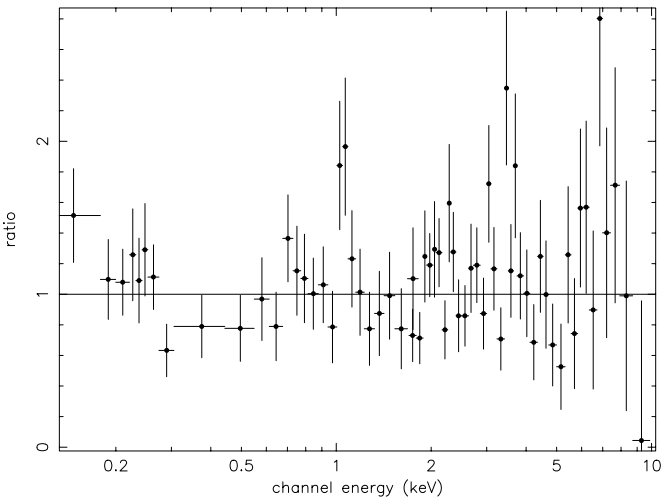

Fig. 11. Data to model ratio for an ionized disk model. The energy is in the observer frame.

The timing analysis revealed the presence of significant flux variations on very small time scales, which lead to an extreme value ($\eta > 2$) for the efficiency in the conversion of gravitational potential energy into X-ray emission. Although large amplitude variability on short time scales is a common feature among NLS1 galaxies, up to now a similar extreme behaviour was observed only in PKS 0558-504 (Remillard et al. 1991), and was attributed to relativistic beaming occurring in the jet, given the radio-loud nature of this source. RX J1702.5+3247 was detected in the FIRST VLA radio survey, but is formally defined as a radio–quiet source, on the basis of the radio-to-optical flux ratio R. On the other hand, the extreme value of η indicates the presence of beaming effects, which might be naturally explained by the existence of a relativistic jet albeit here in a radio–quiet object. This scenario has already been proposed for radio-intermediate quasars on the basis of VLBI observations and brightness temperature calculations (e.g. Falke et al. 1996). Such a hypothesis finds further support in recent VLBA radio observations of Seyfert galaxies, where sub-relativistic jets on parsec-scale were detected (e.g. Ulvestad et al. 1999) and in one case (III Zw 2; Brunthaler et al. 2000) even superluminal motion was measured. An alternative explanation is that the fast variability is related to strong relativistic effects occurring in the accretion disk seen under large viewing angles (namely an edge–on disk; see e.g. Cunningham 1975). However this interpretation seems to be in conflict with the large equivalent width of the iron Kα fluorescent line, which is expected to decrease rapidly with increasing inclination angles due to relativistic effects (Matt et al. 1992).

The analysis of the spectral properties of RX J1702.5+3247 suggests (at a confidence level between 68% and 90%) the presence of a Kα fluorescent iron emission line. The centroid energy of this line is poorly determined, but is inconsistent with the bulk of the line being produced by iron in a ionization state lower than He-like. It should be noted that high energy iron Kα features have already been detected in two other NLS1 galaxies, Ton S 180 and Ark 564, observed with BeppoSAX (Comastri et al. 1998, 2001), by fitting ionized reflection and absorption models, whose limits have been outlined by Ballantyne et al. (2001). The last authors successfully fit the ASCA data of Ton S 180 and

Ark 564, among other NLS1 spectra, with the Ross & Fabian reflection model, but without finding any emission line consistent with highly ionized iron. Therefore RX J1702.5+3247 is the first object where evidence for a strongly ionized accretion disk is twofold. First, a Gaussian line at energy consistent with that of iron in highly ionized state is required in any spectral model for a significant improvement of the fit. Furthermore, the joint LECS+MECS spectrum is well fitted by the Ross & Fabian ionized disk reflection model with a high ionization parameter ($\xi \sim 2500$).

The present results fit fairly well with the hypothesis that NLS1 have higher accretion rates, relative to the Eddington value, compared to normal broad line Seyfert galaxies. In fact, high accretion rates are accompanied by strong ionization of the disk surface layers. According to the hypothesis of higher accretion rates and consequently smaller black hole masses (provided that the energy conversion efficiency is the same), the steep soft excess is explained by the shift of the accretion disk spectrum into the soft X-ray band. The strong flux of soft photons could lead to a strong Compton cooling in the corona and thus to a steep hard tail. Despite the rather steep soft photon index ($\Gamma = 3.37$ in the ROSAT observation), RX J1702.5+3247 shows only a weak soft excess, confined to the very soft part (<0.3 keV) of the X-ray spectrum. However, the lack or weakness of the soft component is not uncommon among NLS1 galaxies, as noted by Leighly (1999b), who also found that the soft excess strength is related to the differences in the relative normalizations of the soft excess component and the power law, rather than to the difference in the slopes of the soft and hard band power laws.

Acknowledgements. We thank the anonymous referee for the useful comments and suggestions that improved the paper. MG acknowledges support from the European Commission under contract number ERBFMRX-CT98-0195 (TMR network "Accretion onto black holes, compact stars and protostars"). SALM acknowledges support from NSF grant AST-98-02791 and from the Institute of Geophysics and Planetary Physics (operated under the auspices of the U.S. Department of Energy by Lawrence Livermore National Laboratory under contract No. W-7405-Eng-48).

References

Bade, N., Fink, H. H., Engels, D., et al. 1995, A&AS, 110, 469
Ballantyne, D. R., Iwasawa, K., & Fabian, A. C. 2001, MNRAS, in press [astro-ph/0011360]
Becker, R. H., White, R. L., & Helfand, D. J. 1995, ApJ, 450, 559
Boella, G., Butler, R. C., Perola, G. C., et al. 1997a, A&AS, 122, 299
Boella G., Chiappetti L., Conti G., et al., 1997b, A&AS, 122, 327
Boller, Th., Brandt, W. N., & Fink, H. H. 1996, A&A, 305, 53
Boller, Th., Brandt, W. N., Fabian, A. C., & Fink, H. H. 1997, MNRAS, 289, 393
Boroson, T. A., & Green, R. F. 1992, ApJS, 80, 109
Brandt, W. N., Mathur, S., & Elvis, M. 1997, MNRAS, 285, 25
Brandt, W. N., Boller, Th., Fabian, A. C., & Ruszkowski, M. 1999, MNRAS, 303, L53
Brinkmann, W., Laurent-Muehleisen, S. A., Voges, W., et al. 2000, A&A, 356, 445
Brunthaler, A., Falcke, H., Bower, G. C., et al. 2000, A&A, 357, L45.
Comastri, A., Fiore, F., Guainazzi, M., et al. 1998, A&A, 333, 31
Comastri, A., Stirpe, G. M., Vignali, C., et al. 2001, A&A, in press [astro-ph/0010476]
Cunningham, C. T. 1975, ApJ, 202, 788
Dickey, J. M., & Lockman, F. J. 1990, ARA&A, 28, 215
Fabian, A. C. 1979, Proc. R. Soc. London, Ser. A, 366, 449
Falke, H., Patnaik, A. R., & Sherwood, W. 1996, ApJ, 473, L13
Fiore, F., Laor, A., Elvis, M., Nicastro, F., & Giallongo, E. 1998, ApJ, 503, 607
Fiore, F., Guainazzi, M., & Grandi, P. 1999, Handbook for BeppoSAX NFI spectral analysis
Forster, K., & Halpern, J. P. 1996, ApJ, 468, 565
Grupe, D., Leighly, K. M., Thomas, H.-C, & Laurent-Muehleisen, S. A. 2000, A&A, 356, 11
Grupe, D., Thomas, H.-C, & Beuermann, K. 2001, A&A, in press
Haardt, F., & Maraschi, L. 1993, ApJ, 413, 507
Haardt, F., Maraschi, L., & Ghisellini, G. 1994, ApJ, 432, L95
Laor, A. 1991, ApJ, 376, 90
Laor, A., Fiore, F., Elvis, M., et al. 1997, ApJ, 477, 93
Leighly, K. M. 1999a, ApJS, 125, 297
Leighly, K. M. 1999b, ApJS, 125, 317
Matt, G., Perola, G. C., Piro, L., & Stella, L. 1992, A&A, 257, 63, Erratum, 263, 453
Nayakshin, S., Kazanas, D., & Kallman, T. R. 2000, ApJ, 537, 833
Osterbrock, D. E., & Pogge, R. W. 1985, ApJ, 297, 166
Parmar, A. M., Martin, D. D. E., Bavdaz, M., et al. 1997, A&AS, 122, 309
Pfeffermann, E., Briel, U. G., Hippmann, H., et al. 1986, SPIE, 733, 519
Pounds, K. A., Done, C., Osborne, J. P. 1995, MNRAS, 277, L5
Remillard, R. A., Grossman, B., Bradt, H. V., et al. 1991, Nature, 350, 589
Ross, R. R., & Fabian, A. C. 1993, MNRAS, 261, 74
Ross, R. R., Fabian, A. C., & Young, A. J. 1999, MNRAS, 306, 461
Siebert, J., Leighly, K. M., Laurent-Muehleisen, S. A., et al. 1999, A&A, 348, 678
Stocke, J. S., Morris, S. L., Weymann, R. J., & Foltz, C. B. 1992, ApJ, 396, 487
Trümper, J. 1983, Adv. Space Res., 4, 241
Turner, T. J., George, I. M., & Nandra, K. 1998, ApJ, 508, 648
Ulvestad, J. S., Antonucci, R. R. J., & Goodrich, W. 1995, AJ, 109, 81
Ulvestad, J. S., Wrobel, J. M., Roy, A. L., et al. 1999, ApJ, 517, L81
Voges, W., Aschenbach, B., Boller, Th., et al. 1999, A&A, 349, 389
White, R. L., Becker, R. H., Gregg, M. D., et al. 2000, ApJS, 126, 133
Zimmermann, H.-U., Boese, G., Becker, W., et al. 1996, EXSAS USER's GUIDE, http://wave.xray.mpe.mpg.de/exsas